

QUANTIFYING THE HYDROGEN EMBRITTLEMENT OF PIPE STEELS FOR SAFETY CONSIDERATIONS

Briottet L.¹, Moro, I.², Lemoine, P.³

¹CEA, LITEN, DTBH, LCTA, F-38054 Grenoble, France, laurent.briottet@cea.fr.

²CEA, LITEN, DTBH, LCTA, F-38054 Grenoble, France, isabelle.moro@cea.fr.

³CEA, LITEN, DTBH, LCTA, F-38054 Grenoble, France, patrick.lemoine@cea.fr.

ABSTRACT

In a near future, with an increasing use of hydrogen as an energy vector, gaseous hydrogen transport as well as high capacity storage may imply the use of high strength steel pipelines for economical reasons. However, such materials are well known to be sensitive to hydrogen embrittlement (HE). For safety reasons, it is thus necessary to improve and clarify the means of quantifying embrittlement. The present paper exposes the changes in mechanical properties of a grade API X80 steel through numerous mechanical tests, i.e. tensile tests, disk pressure test, fracture toughness and fatigue crack growth measurements, WOL tests, performed either in neutral atmosphere or in high-pressure of hydrogen gas. The observed results are then discussed in front of safety considerations for the redaction of standards for the qualification of materials dedicating to hydrogen transport.

INTRODUCTION

Due to the development of technologies based on hydrogen as an energy vector, it is necessary to build substructures for hydrogen production, transport, storage and conversion. Pipelines could be a convenient way to transport large quantities of hydrogen through great distances. For cost reduction purpose, high strength steels are good candidates although it is known that Hydrogen Embrittlement (HE) susceptibility increases with material mechanical properties [1]. Nowadays, there is no safety standard to choose materials for hydrogen pipelines. Thus, the knowledge of hydrogen effect must be improved to appropriately select material for pipelines fabrication dedicated to hydrogen transport. Many types of mechanical tests under hydrogen can be performed and, as will be shown in this paper, depending on the testing conditions, hydrogen embrittlement can be considered low or high.

From this perspective, the present paper exposes a study realized on a high strength steel grade API X80 in hydrogen or neutral gas. Various mechanical tests were used in order to fully investigate the effect of gaseous hydrogen on mechanical and fracture properties. Indeed, extensive studies realized during the last 50 years clearly demonstrated that hydrogen may affect materials through a great extent, depending on experimental conditions and microstructure considerations [2]. Studying ferritic and martensitic steels, it was demonstrated that the greatest effect of hydrogen gas on mechanical properties is to induce a loss of elongation to failure, while the yield and the ultimate stresses are usually unchanged [3]. It was also observed that, for steels which exhibit a ductile fracture in neutral gas, brittle failure occurs in hydrogen environment and quasi-cleavage appears on the fracture surfaces [4]. Lastly, it was shown that HE is greatly susceptible to experimental conditions (temperature, strain rate...), as well as on the way of hydrogen charging. Indeed, cathodic charging may bring high quantities of hydrogen in materials without considerations of surface limitations due to the oxide layers thus inducing great material damages such as hydrogen blistering. On the opposite, gaseous hydrogen charging, even at high pressure, can not introduce such quantities of hydrogen into metals and induces embrittlement based on other mechanisms such as HIDE [4], HELP [5-7], AIDE [4] or HESIVE [8, 9].

In the present work, tensile tests, disk pressure tests and fracture mechanic tests (Fracture toughness and fatigue crack growth measurements, WOL tests) were realized and compared. While the used material and the experimental procedures are exposed in the first part of this paper, the second one addresses the observed effects of hydrogen on the X80 mechanical properties and damage. Lastly, the experimental procedures and obtained results are compared and discussed in front of safety considerations for materials dedicated to hydrogen transport.

1.0 MATERIAL AND EXPERIMENTAL PROCEDURES

1.1 Material

The studied material is a high-strength steel grade API X80 traditionally used for pipelines manufacturing. It was received as a piece of pipeline with an external diameter of 914mm and a thickness of 11mm. Its chemical composition is given in Table 1. To evaluate its mechanical properties, smooth axisymmetric specimens (gage length 30mm, diameter 6mm) were machined along the pipeline longitudinal direction. Tensile tests were conducted in air at room temperature and at $5 \times 10^{-5} \text{ s}^{-1}$. The results are presented in Table 2. Additionally tensile tests were also conducted at 0.55 s^{-1} and did not revealed any significant effect of strain rate on X80 mechanical properties. As shown in Fig. 1a, for all these tensile tests the corresponding fracture surfaces exhibit dimples.

Table 1. Concentration range for alloy elements in API grade X80 steel (%wt).

C	Mn	Si	Nb	V	Cu	P	S	Fe
0.075	1.86	0.35	0.05	<0.01	0.22	0.015	<0.003	Bal.

Table 2. Mechanical properties of X80 steel along the longitudinal direction.

Ultimate stress (MPa)	Yield stress (MPa)	Young modulus (GPa)	Elongation to failure (%)
677	507	209	26

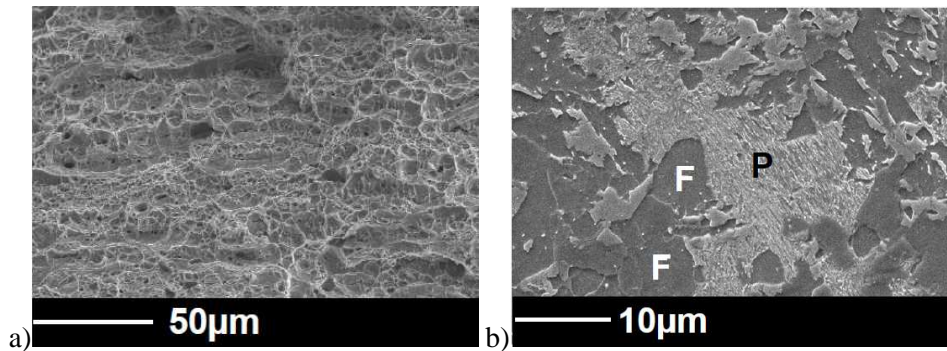


Figure 1. Fracture surface of tensile specimens tested in air at room temperature and $5 \times 10^{-5} \text{ s}^{-1}$ (a) SEM examination of X80 microstructure (b). F = Ferrite. P = Pearlite.

The X80 microstructure was studied through SEM observations on polished specimens (1200 Sic grade paper, $6 \mu\text{m}$ and $3 \mu\text{m}$ diamante solutions) chemically attacked using a 5% concentrated Nital solution during 7s. The ferrite grain size is about $10 \mu\text{m}$ while that of the pearlite phase ranges from $5 \mu\text{m}$ to $20 \mu\text{m}$ (Fig. 1b). Moreover, the material has a strong microstructural anisotropy with pearlite alignments along the rolling direction.

1.2 Tensile tests

Tensile tests in hydrogen gas were performed at room temperature, with a servo hydraulic apparatus and a 100kN load sensor and using the same specimen geometry as in air. They were conducted in a pressure vessel filed up with hydrogen or nitrogen gas up to 30MPa and for strain rates ranging from $5.5 \times 10^{-7} \text{ s}^{-1}$ to 0.55 s^{-1} . For tests in hydrogen gas, the pressure vessel is first filled up with nitrogen, then a primary vacuum is realized. High purity hydrogen (N60) is finally introduced. The same procedure is repeated for all tests in order to ensure reproducibility.

1.3 Disk pressure tests

This test [10, 11] is used for material qualification dedicating to hydrogen storage in seamless bottle following the ISO standard 11114-4:2008. It consists in loading an embedded disk with an increasing pressure of helium or hydrogen gas for various pressure rates (Fig. 2). Then, the ratio I_E of failure pressures in helium and in hydrogen at a given pressure rate is calculated. The great feedback of material behaviors during service life in hydrogen gas led to the conclusion that the material is accepted for hydrogen storage when this ratio is lower than 2.

Disks (diameter 58mm, thickness 0.75mm) were machined in the middle of the X80 sheet with the disk axis perpendicular to the sheet thickness. Before a test, they were manually polished using a 1200SiC grade paper to ensure similar surface states. Roughness was then measured and showed a good reproducibility with an average value of $0.15\mu\text{m}$. The disks were then cleaned in ethanol using ultrasounds.

Tests were performed at room temperature for pressure increasing rates up to $250\text{MPa}\cdot\text{min}^{-1}$ using helium or hydrogen gas.

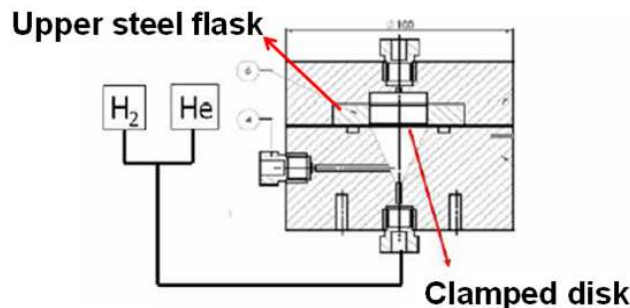


Figure 2. Scheme of the Disk Pressure Test.

1.4 Fracture toughness and fatigue crack growth measurements

Specimens were machined according to the Compact Tension geometry (Fig. 3) with the precrack starter notch perpendicular to the transverse direction and the crack propagation along the longitudinal direction of the pipeline.

For all specimens, a precrack was propagated by applying cyclic loading in air, at room temperature and with a load frequency of 10Hz and a load ratio of 0.1. Precrack tests were conducted with a decreasing load in order to reach a stress intensity factor value of $34\text{MPa}\cdot\text{m}^{0.5}$ at the start of the precrack and a $24\text{MPa}\cdot\text{m}^{0.5}$ value at the end. The total final precrack lengths ranged between 2mm and 3mm for specimens dedicating to fracture toughness measurements, and between 8mm and 9mm for fatigue crack growth measurements.

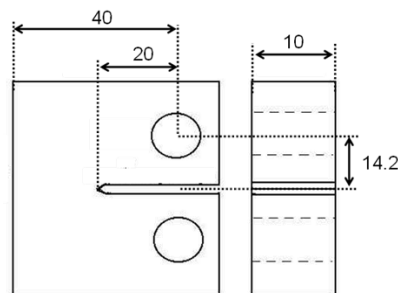


Figure 3. Compact Tension specimen geometry.

Before fracture toughness or fatigue crack growth measurements, specimens were cleaned in ethanol with ultrasound. The apparatus used for mechanical loading was the one previously described for tensile tests.

Concerning the fracture toughness measurements, realized according to ISO 12135, tests were performed using the multi-specimens method, i.e. the crack length is measured at the end of the test. Pressure vessel was either filled up with 30MPa of hydrogen or nitrogen gas at room temperature and the tests were conducted at $0.1\text{mm}\cdot\text{min}^{-1}$.

The fatigue crack growth tests were performed at room temperature. The specimens were subjected to cyclic loading with a load ratio of 0.1 and for a frequency of 10Hz for tests in air and of 0.1Hz for the test in hydrogen gas. Crack growth measurements were realized using a compliance method following the crack opening displacement. The stress intensity factors addressed during the tests range approximately between $10\text{MPa}\cdot\text{m}^{0.5}$ and $70\text{MPa}\cdot\text{m}^{0.5}$.

1.5 WOL tests

The WOL tests were performed, by Air Liquide within the French ANR CATHY-GDF project, using the Compact Tension specimen geometry previously exposed in Fig. 3. Following the standard ISO 7539-6, precrack was conducted by cyclic loading in air with a load ratio of 0.1 and a frequency of 95Hz. The last 10^4 cycles were performed with a decreasing stress intensity factor. The precrack was realized using a servo hydraulic Instron 20kN apparatus.

Once precracked, specimens were loaded in air to obtain a stress intensity factor ranging from $39\text{MPa}\cdot\text{m}^{0.5}$ to $111\text{MPa}\cdot\text{m}^{0.5}$. Then, they were introduced in a pressure vessel at room temperature filled up with 30MPa of hydrogen gas. After 1000 hours, the crack lengths were measured.

A similar test has also been performed with a specimen precracked in air but mechanically loaded with a stress intensity factor of $90\text{MPa}\cdot\text{m}^{0.5}$ in 30MPa of hydrogen gas. In that case, the crack propagation has been measured after seven days.

2.0 EXPERIMENTAL RESULTS

2.1 Hydrogen effect on mechanical properties, fracture toughness and fatigue crack growth

Tensile results in 30MPa of hydrogen gas shown that hydrogen unchanged the young modulus, the yield stress, the ultimate tensile stress nor the strain hardening. On the opposite, the material exhibits a strong loss of ductility increasing with a decreasing strain rate, as shown in Fig. 4. The influence of hydrogen pressure from 0.1MPa to 30MPa has been addressed by performing tensile tests at $5\times 10^{-5}\text{s}^{-1}$. Hydrogen embrittlement, in terms of ductility, increases when pressure increases up to a threshold pressure around 5MPa [12]. Above this pressure, HE does not increase.

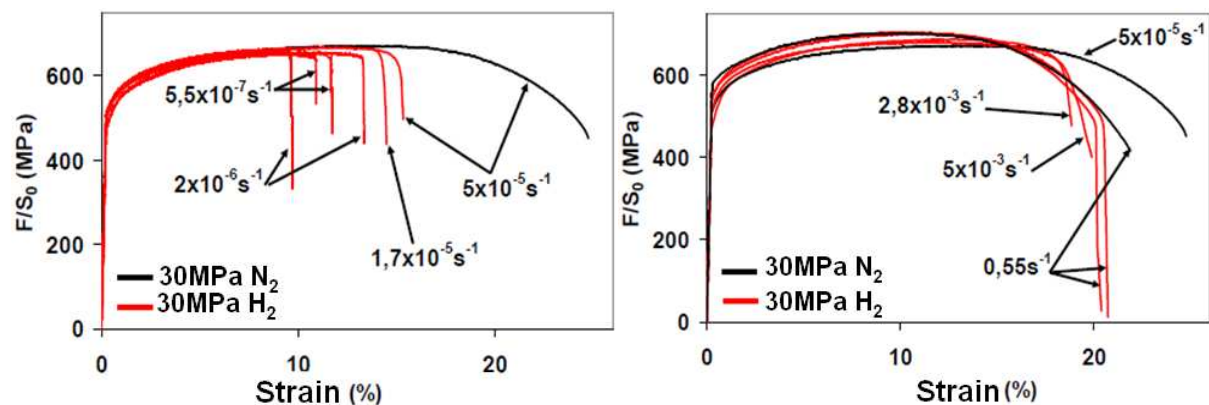


Figure 4. Tensile tests in 30MPa of hydrogen or nitrogen gas for various strain rates.

The DPT results are given in Fig. 5. The embrittlement index I_E is lower than 2 with the exception of one single test realized at low value of dP/dt . In this case, the disk did not burst but a crack was found after the test was completed. It is worth noting that in our device, rupture is detected by the measure of a downstream pressure. Some other devices detect rupture by measuring the upstream decrease of pressure rate. It is yet not clear whether these two methods always lead to the same results.

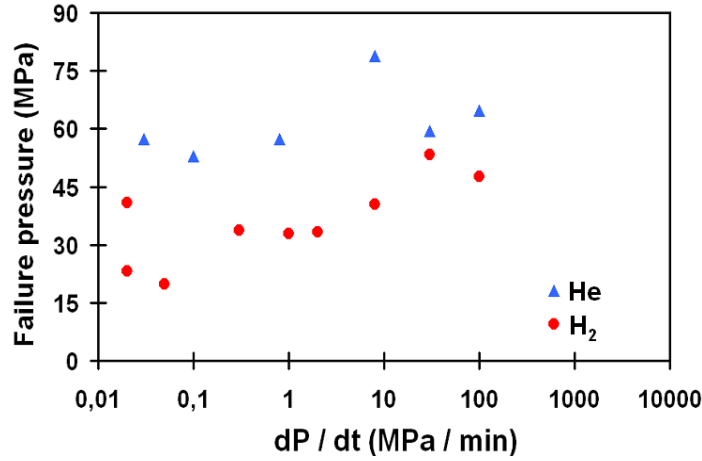


Figure 5. Disk Pressure Tests results.

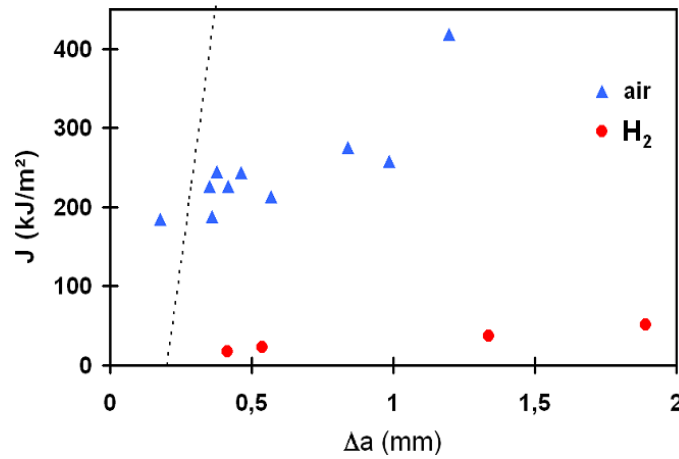


Figure 6. Fracture toughness measurements realized on X80 CT specimens.

The fracture toughness measurements performed in air or in 30MPa of hydrogen are displayed in Fig. 6. A strong decrease of the material toughness, evaluated through the J integral at 0.2mm, is observed in hydrogen. Indeed, it falls from 210kJ.m⁻² in air to 15kJ.m⁻² in 30MPa of hydrogen gas.

In Fig. 7, the crack growth per cycle da/dn is plotted versus the stress intensity factor range ΔK . The coefficients of the Paris law (Eq. 1) fitted on these results are given in Table 3.

$$\frac{da}{dn} = C\Delta K^m \quad (1)$$

Table 3. Paris law parameters

Environment	C (mm.cycle ⁻¹)	m
Air	5x10 ⁻⁹	3.1
30MPa H ₂	2x10 ⁻⁹	4.4

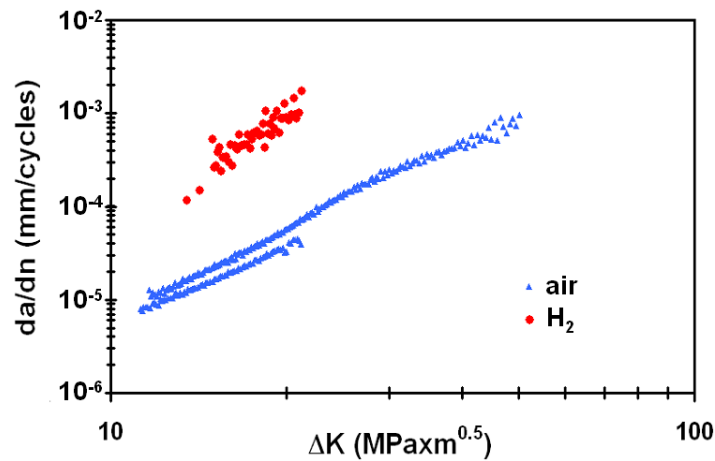


Figure 7. Fatigue crack growth behaviour in air and in 30MPa of hydrogen gas.

Typically, for a ΔK value of $15\text{MPa}\cdot\text{m}^{0.5}$, the crack growth increment per cycle is equal to $2.2 \times 10^{-5}\text{mm}\cdot\text{cycle}^{-1}$ in air and to $3 \times 10^{-4}\text{mm}\cdot\text{cycle}^{-1}$ in 30MPa of hydrogen gas, demonstrating that crack growth increment per cycle is about 10 times higher in gaseous hydrogen than in neutral atmosphere. This effect of hydrogen on crack growth confirms results previously presented in the literature for similar steels [13].

On the opposite of all the previously exposed experimental results which clearly demonstrate the X80 steel hydrogen susceptibility, the WOL tests results did not show any effect of hydrogen. Whatever the stress intensity factor (ranging from $39\text{MPa}\cdot\text{m}^{0.5}$ to $111\text{MPa}\cdot\text{m}^{0.5}$), no crack growth was measured at the end of the 1000hours hydrogen exposure. Note that for the test mechanically loaded in hydrogen gas, no crack growth was observed either.

2.2 Fracture surfaces and material damages in hydrogen gas

To complete this mechanical analysis, optical and SEM observations of the fracture surfaces were realized. As described in the paragraph 1.1 and shown by Fig.1, the fracture surfaces of the specimens tested in neutral atmospheres always exhibit a ductile appearance whatever the loading conditions (tensile, disk or CT specimens).

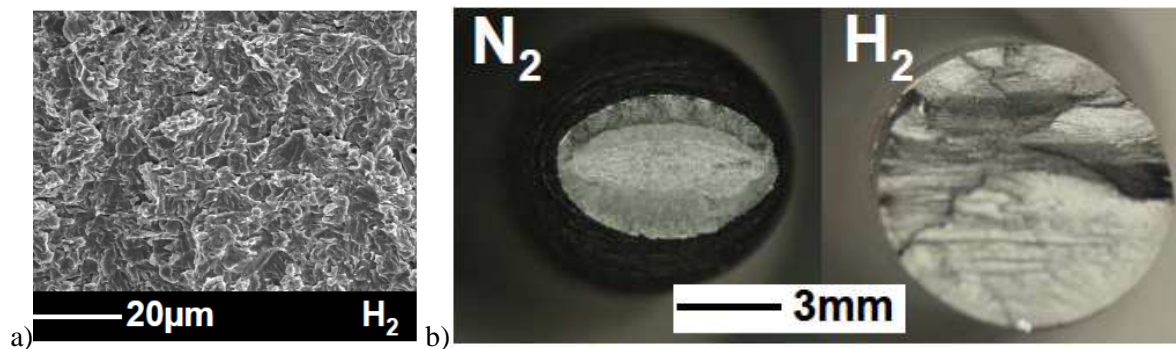


Figure 8. Typical fracture surface in hydrogen gas (SEM examination) (a) and optical examination of tensile specimens strained at $5 \times 10^{-5}\text{s}^{-1}$ in 30MPa of nitrogen or hydrogen gas (b).

When tested in hydrogen, the tensile and CT specimens show a brittle failure and exhibit a typical quasi-cleavage appearance (Fig. 8a). The examinations of tensile specimens failed in hydrogen revealed several types of damage. First, necking is strongly reduced (Fig. 8b). Second, delamination along the pearlite alignments is highly enhanced by hydrogen (Fig.8a and Fig.10). Third, the external surfaces of the specimens tested in hydrogen display numerous external cracks perpendicular to the

tensile direction (Fig. 9a), the density of which increases with the plastic strain. These cracks are not observed on the specimens failed in neutral atmosphere.

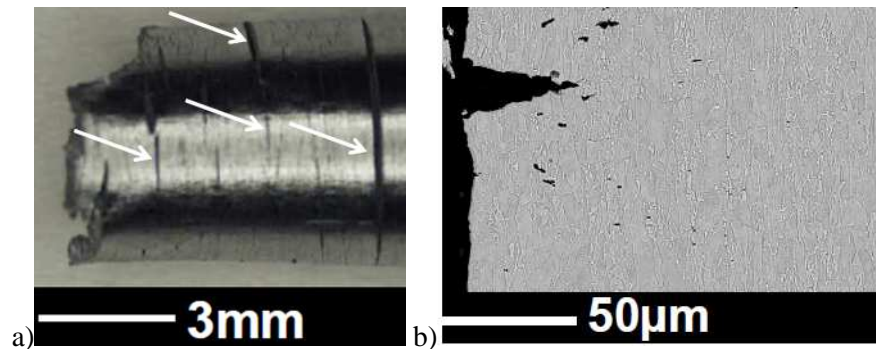


Figure 9. External surface of a tensile specimen strained in 30MPa hydrogen (a) SEM examination of a longitudinal section of a specimen strained in 30MPa of hydrogen at $5 \times 10^{-5} \text{ s}^{-1}$ (b).

Moreover, SEM analysis of longitudinal sections of specimens failed in hydrogen revealed numerous micro-cracks located in pearlite phases, and perpendicular to the tensile direction. They are mainly located in the area of localised plasticity at the tip of the external macrocracks (Fig. 9b).

In Fig. 10 concerning fracture toughness measurements, fractographies of the specimens tested in nitrogen or in hydrogen gas are displayed. The crack propagation for a given crack opening displacement is much longer in hydrogen than in air, in accordance with the observed large toughness decrease.

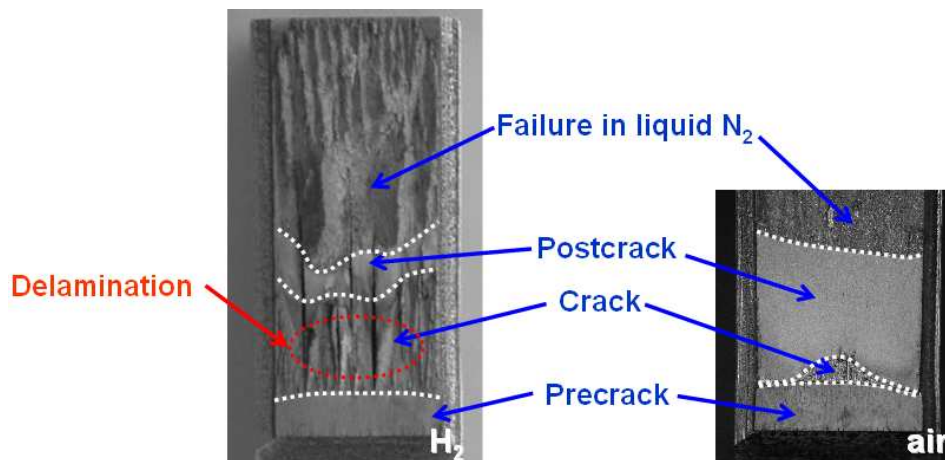


Figure 10. Crack propagation during the toughness multispecimens method in air (right) or in 30MPa of hydrogen gas (left) for a same initial crack length and a same final crack opening displacement.

The *post-mortem* SEM examination of disk loaded in hydrogen gas revealed that their fracture surfaces were split in two areas, as exposed in Fig. 11. The area (area 1 in Fig. 11) in contact with hydrogen is brittle exhibiting quasi-cleavage. On the opposite side of the disk, the second area (area 2 in Fig. 11) is fully ductile.

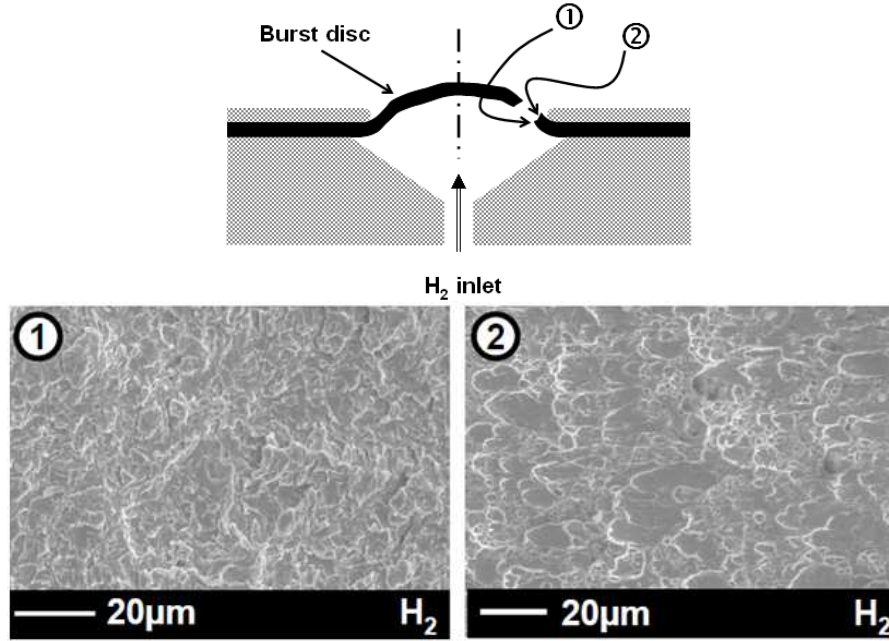


Figure 11. Fracture surface of disk tested in hydrogen gas at 20MPa.min⁻¹.

Finally, SEM examinations performed by Air Liquide on CT specimens tested according to the WOL procedure did not reveal any evidence of HE on the fracture surfaces.

3.0 DISCUSSION

The mechanical behaviour of X80 in high-pressure of hydrogen gas demonstrated that hydrogen promotes several types of damage, such as external or pearlite located phases. It is then possible to define many embrittlement indexes depending on the loading conditions:

- Hydrogen induces a significant loss of elongation to failure on tensile specimen which may be quantified by :

$$I_{EF}(\%) = \frac{E_F^{N_2} - E_F^{H_2}}{E_F^{N_2}} \times 100 \quad (2)$$

where $E_F^{N_2}$ - Elongation to failure in nitrogen gas; $E_F^{H_2}$ - Elongation to failure in hydrogen gas.

- The decrease of the fracture toughness can be quantified by the following index :

$$I_J(\%) = \frac{J^{N_2} - J^{H_2}}{J^{N_2}} \times 100 \quad (3)$$

where J^{N_2} - X80 fracture toughness in nitrogen gas, J.m⁻²; J^{H_2} - X80 fracture toughness in hydrogen gas, J.m⁻².

- Hydrogen strongly increases the crack growth increments per cycle which is evaluated through the following index :

$$I_{CG}(\%) = \left(1 - \frac{(da/dn)_{He}}{(da/dn)_{H_2}} \right) \times 100 \quad (4)$$

where $\left(\frac{da}{dn}\right)_{He}$ - Crack growth increment per cycle in helium, mm.cycle⁻¹; $\left(\frac{da}{dn}\right)_{H_2}$ - Crack growth increment per cycle in hydrogen, mm.cycle⁻¹.

- Hydrogen decreases the failure pressure noticed through DPT thus indicating HE. This embrittlement can be quantified by an index based upon the above described failure ratio I_E :

$$I_{DPT}(\%) = \frac{P^{He} - P^{H_2}}{P^{He}} \times 100 = \left(1 - \frac{1}{I_E}\right) \times 100 \quad (5)$$

where P^{He} - Failure pressure in helium for a given (dP/dt) value, Pa; P^{H_2} - Failure pressure in hydrogen for a similar (dP/dt) value, Pa; I_E - Embrittlement index defined following ISO 11114-4 (For $I_E = 2$, $I_{DPT} = 50\%$).

- Let define such an index for the WOL test as follows :

$$I_{WOL}(\%) = \frac{\Delta a_{H_2}}{(W - a_o)} \times 100 \quad (6)$$

where (W-a_o) - Remaining ligament after initial mechanical loading, m; Δa_{H_2} - crack propagation under hydrogen, m.

These indexes have been defined in order to range between 0 and 100%, the latter corresponding to the highest possible hydrogen susceptibility. Note that in between, it is not possible to compare quantitatively the obtained values since the ways damage is monitored are too different. Moreover, other indexes based on the specimen surface analysis could also be proposed: ratio of the brittle to ductile surfaces, number or sizes of cracks along the gage length, etc.

These various indexes have been estimated from the above-mentioned tests and are displayed in Fig. 12. First, let consider specimens without initial defects, i.e. tensile as well as disk tests. I_{EF} and I_{DPT} values are similar and can measure the influence of the loading rate or the increasing pressure rate. Indeed, for either tensile or disk pressure tests performed at low strain rates or (dP/dt) values, i.e. respectively $2 \times 10^{-6} s^{-1}$ and $0.02 MPa \cdot min^{-1}$, the I_{EF} and I_{DPT} values are around 62%. Similarly, at high strain rate or (dP/dt) values, i.e. respectively $0.55 s^{-1}$ and $100 MPa \cdot min^{-1}$, I_{EF} and I_{DPT} values are both equal to about 18%. Second, the indexes derived from toughness or fatigue crack growth tests are similar and close to one.

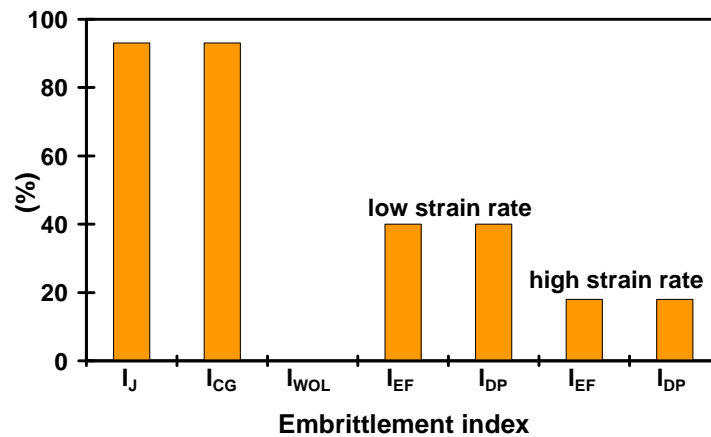


Figure 12. Some embrittlement indexes of X80 steel

Finally, the index derived from the WOL test indicated no hydrogen susceptibility. In the latter test, the specimen contains a crack and is charged either in air or in 30MPa of hydrogen gas and then kept statically loaded under hydrogen gas pressure.

Depending on the loading conditions – mainly static or dynamic loading under hydrogen, presence or not of a geometrical defect – the various measures of hydrogen embrittlement will describe a large as well as no embrittlement. This can be a real problem since some of these tests are proposed in the same standard (ISO 11114-4:2008).

While dynamic tests demonstrate a clear influence of hydrogen on X80 mechanical properties and damages, static tests do not reveal any HE. This major difference can be explained by two effects: the influence of an oxide layer on the specimen surface or at the crack tip, and interactions between hydrogen and dislocations. Indeed, the WOL specimens were precracked and loaded in air (except for one specimen). The oxide layer developed on the crack surface will hinder hydrogen adsorption and absorption on the material, thus providing X80 from HE [14]. On the contrary, during dynamic loading in hydrogen, this oxide layer is broken, promoting hydrogen adsorption and absorption. The second assumption deals with interactions between hydrogen and dislocations. It is well known that dislocations promote hydrogen transport through the material [15]. Moreover, mechanisms such as HELP or AIDE are based on the fact that hydrogen favours high-densities dislocation piles-up by increasing planar slip, decreasing the interaction energy between dislocations and activating Frank-Read sources [4]. While new dislocations are continuously created during dynamic tests, in static tests the dislocation density remains constant after the initial mechanical loading.

Concerning the dynamic tests, it is observed that the fracture mechanic tests, i.e. fracture toughness and fatigue crack growth measurements, demonstrate a higher HE susceptibility than DPT and tensile tests. This is directly linked to the hydrogen content in the material. Indeed, usual models of hydrogen diffusion [16] clearly express that the total hydrogen concentration, i.e. lattice and trapped hydrogen, is increased by positive hydrostatic stress σ_H and by plastic strain ϵ_p (as measured for X80 in [17]). In presence of a geometrical defect, the values of σ_H and ϵ_p are greatly increased at the notch tip, inducing a higher hydrogen concentration.

The development of large quantity of hydrogen transport and storage will require, for safety reasons, adequate qualification standards. The tests will have to be representative of the service life conditions of such substructure and they also have to be comparable and give similar trends. As shown in this paper, many types of mechanical tests are available under hydrogen, characterizing different hydrogen embrittlement mechanisms. For the redaction of standards for the qualification of materials dedicating to hydrogen energy substructures, full and exhaustive comparative studies between the advised mechanical tests in hydrogen should be conducted. The aim would be to identify the types of mechanical tests relevant to a given application.

Finally, hydrogen susceptibility of welds is also an important issue. Thereupon, the French ANR project CESTAR is partly dedicated to the analysis of fatigue crack propagation in welds of ferrite perlite steels.

ACKNOWLEDGMENTS

The authors acknowledge the French National Agency for Research for partial funding of this work within the CATHY-GDF as well as CESTAR program.

REFERENCES

1. Wang, M., Akiyama, E. and Tsuzaki, K., Effect of hydrogen on the fracture behavior of high strength steel during slow strain rate test, *Corrosion Science*, **49**, 2007, pp. 4081-4097.
2. Barthélémy, H., Effects of purity and pressure on the hydrogen embrittlement of steels and others metallic materials, Proceedings of the 3rd International Conference on Hydrogen safety, 16-18 September 2009, Ajaccio, France.

3. Lam, P.S., Gaseous hydrogen effects on the mechanical properties of carbon and low alloy steels, Savannah River National Laboratory Report No. WSRC-TR-2006-00119 Rev. 1.
4. Lynch, S.P., Progress towards understanding mechanisms of hydrogen embrittlement and stress corrosion cracking, Proceedings of the NACE International Corrosion Conference, 11-15 March 2007, Nashville, USA.
5. Ferreira, P.J., Robertson, I.M. and Birnbaum, H.K., Hydrogen effects on the character of dislocations in high-purity aluminium, *Acta Materialia*, **47**, No. 10, 1999, pp. 2991-2998.
6. Nibur, K.A., Bahr, D.F. and Somerday, B.P., Hydrogen effects on dislocation activity in austenitic steel, *Acta Materialia*, **54**, 2006, pp. 2677-2684.
7. Ferreira, P.J., Robertson, I.M. and Birnbaum, H.K., Hydrogen effects on the interaction between dislocations, *Acta Materialia*, **46**, No. 5, 1998, pp. 1749-1757.
8. Takai, K., Shoda, H., Suzuki, H. and Nagumo, M., Lattice defects dominating hydrogen-related failure of materials, *Acta Materialia*, **56**, No. 18, 2008, pp. 5158-5167.
9. Nagumo, M., Hydrogen related failure of steels - a new aspect, *Materials Science and Technology*, **20**, 2004, pp. 940-950.
10. Fidelle, J.P., The present status of the disk pressure test for Hydrogen Embrittlement, Hydrogen Embrittlement : prevention and control - ASTM STP62 (Raymond, L. Eds.), Philadelphia, 1988, p. 153.
11. Fidelle, J.P., Broudeur, R. and Roux, C., Hydrogen gas embrittlement under the influence of strain rate, temperature and thickness effects - Relationship with delayed failure, Proceedings of the International Conference on the effect of hydrogen on materials, 7-11 September 1995, Jackson Lake, USA.
12. Moro, I., Briottet, L., Lemoine, P., Andrieu, E., Blanc, C., Odemer, G., Chêne, J. and Jambon, F., Damage under high-pressure hydrogen environment of a high strength pipeline steel X80, Proceedings of the International Conference on the effect of hydrogen on materials, 7-10 september 2008, Jackson Lake, USA.
13. Somerday, B.P., Nibur, K.A. and San Marchi, C., Measurements of fatigue crack growth rate for steels in hydrogen containment components, Proceedings of the 3rd International Conference on Hydrogen safety, 16-18 September 2009, Ajaccio, France.
14. Tison, P., Influence de l'hydrogène sur le comportement des matériaux, Ph.D, Université Pierre et Marie Curie (France), 1983.
15. Chêne, J. and Brass, A.M., Hydrogen Transport by mobile dislocations in Nickel base superalloy single crystals, *Scripta Materialia*, **40**, No. 5, 1999, pp. 537-542.
16. Taha, A., Sofronis, P., A micromechanics approach to the study of hydrogen transport and embrittlement, *Engineering Fracture Mechanics*, **68**, 2001, pp. 803-837.
17. Moro, I., Briottet, L., Lemoine, P., Andrieu, E., Blanc, C. and Odemer, G., Hydrogen embrittlement susceptibility of a high-strength steel X80, *Materials Science and Engineering*, **A527**, No. 27-28, 2010, pp. 7252-7260.